SCIENTIFIC REPORTS

OPEN

SUBJECT AREAS:
NANOSCALE MATERIALS
MATERIALS FOR ENERGY AND CATALYSIS

Received
23 July 2013

Accepted
2 September 2013

Published
24 September 2013

Correspondence and requests for materials should be addressed to C.Y. (chye@issp.ac.cn)

A Route to Phase Controllable $Cu_2ZnSn(S_{1-x}Se_x)_4$ Nanocrystals with Tunable Energy Bands

Shulin Ji[1], Tongfei Shi[1], Xiaodong Qiu[1], Jian Zhang[1], Guoping Xu[1], Chao Chen[1], Zheng Jiang[2] & Changhui Ye[1]

[1]Key Laboratory of Materials Physics and Anhui Key Laboratory of Nanomaterials and Technology, Institute of Solid State Physics, and Key Laboratory of New Thin Film Solar Cells, Chinese Academy of Sciences, Hefei 230031, P. R. China, [2]Shanghai Synchrotron Radiation Facility, Shanghai Institute of Applied Physics, Chinese Academy of Sciences, Shanghai 201204, P. R. China.

$Cu_2ZnSn(S_{1-x}Se_x)_4$ nanocrystals are an emerging family of functional materials with huge potential of industrial applications, however, it is an extremely challenging task to synthesize $Cu_2ZnSn(S_{1-x}Se_x)_4$ nanocrystals with both tunable energy band and phase purity. Here we show that a green and economic route could be designed for the synthesis of $Cu_2ZnSn(S_{1-x}Se_x)_4$ nanocrystals with bandgap tunable in the range of 1.5–1.12 eV. Consequently, conduction band edge shifted from −3.9 eV to −4.61 eV (relative to vacuum energy) is realized. The phase purity of $Cu_2ZnSn(S_{1-x}Se_x)_4$ nanocrystals is substantiated with in-depth combined optical and structural characterizations. Electrocatalytic and thermoelectric performances of $Cu_2ZnSn(S_{1-x}Se_x)_4$ nanocrystals verify their superior activity to replace noble metal Pt and materials containing heavy metals. This green and economic route will promote large-scale application of $Cu_2ZnSn(S_{1-x}Se_x)_4$ nanocrystals as solar cell materials, electrocatalysts, and thermoelectric materials.

$Cu_2ZnSn(S_{1-x}Se_x)_4$ (CZTSSe, $0 \leq x \leq 1$), composed of earth-abundant and nontoxic elements, have received much attention due to their potential applications in solar cells, electrocatalysts, and thermoelectricity[1–10]. For many of these applications, it is important to synthesize pure-phased nanocrystals with tunable bandgap, and experimentally determine the band position. It is well-known that a suitable band offset between a heterojunction or a homojunction is essential for efficient charge separation and transport[11]. It is possible to build up a rainbow solar cell using CZTSSe nanocrystals of different bandgap and band positions to facilitate light utilization and charge transport[12,13]. In addition, graded band positions benefit construction of efficient electrocatalytic system by changing materials composition which moves the energy band closer to or far from the redox potential. Composition dependant electrocatalytic activity of Zn(S,Se) towards ethanol was reported and was related to shifts in the position of the conduction band edge under various S/Se ratios[14]. Actually, CZTSSe were reported to show comparable or superior electrocatalytic activity than traditional Pt in solar cells as counter electrode towards I^-/I_3^- and S^{2-}/S_n^{2-} redox couples[5,6]. Composition dependant electrocatalytic activity of CZTSSe was also reported[7]. From energy point of view, CZTSSe with ascertained and tunable band positions has important application in new electrocatalytic system meeting energy level alignment requirement. For instance, new redox couples are frequently developed in quantum dot-sensitized solar cells to efficiently generate photocurrent while overpotentials for charge transfers at interfaces could be further suppressed for efficiency enhancement by choosing appropriate electrocatalysts[15]. Another potential application field is thermoelectricity, as structural change arising from cation disorder could limit thermal conductivity while maintaining high electrical conductivity[16,17]. Structural change from kesterite Cu_2ZnSnS_4 (CZTS) to stannite $Cu_2ZnSnSe_4$ (CZTSe) has always been observed and ascribed to cation disorder in the Cu + Zn layer[18]. Besides structural disorder, tunable bandgap and band positions arose from compositionally alloying could benefit thermoelectric performance[19,20], as in the case of p-type $PbTe_{1-x}Se_x$ alloys[21]. Therefore, CZTSSe nanocrystals with tunable bandgap and band positions may function well as thermoelectric materials.

However, developing a facile and mild one-step method to synthesize CZTSSe nanocrystals with controllable x values and tunable energy band is still a challenging task due to the difficulty in controlling both the phase purity and the composition. Recently, Riha and coworkers have synthesized CZTSSe nanocrystals with the bandgap in the range of 1.47–1.54 eV[22]. CZTSSe nanocrystals with bandgap tunable from 1.0 to 1.5 eV have been synthesized using octadecene as solvent[23]. Up to now, synthesis of CZTSSe nanocrystals by the colloid chemical method has

generally adopted oleylamine (OLA) as the main solvent[3,10,22,23]. OLA is indeed a benchmark solvent for synthesizing uniform, monodispersed, and phase pure nanocrystals ranging from metals to various semiconductors. However, the high production cost and the difficulty in ligand exchange involved in the usage of OLA during the synthesis processes calls for extensive research work. Recently, Talapin group have carried out systematic work on improving device performances through additional surface modification of OLA-capped nanocrystals[24,25]. As suggested by Sargent and coworkers in a recent paper, ligand exchange had better be carried out in solution and a single step film deposition is favored[26]. In this paper, we report on a solution route synthesis of compositionally tunable CZTSSe nanocrystals by employing glycerol as the main solvent. We aim to investigate the possibility to replace OLA with cost effective solvent which is easier to remove during the purification step. Pure-phased CZTSSe nanocrystals in their complete composition range could be obtained with a maximum volume percent of OLA of 20–30%. We for the first time experimentally determined the band position of CZTSSe nanocrystals. Bandgap value could be tuned in the range of 1.5–1.12 eV and conduction band edge shifted from −3.9 eV to −4.61 eV (relative to vacuum energy). Electrocatalytic test of untreated CZTS nanocrystals verifies their superior activity than that of noble metal Pt. As-synthesized CZTSe nanocrystals have thermoelectric ZT value of ~0.35 at 500°C, which have great potential of replacing bulk and heavy metal containing thermoelectric materials. This paves the way for application of CZTSSe nanocrystals in low cost electronic devices.

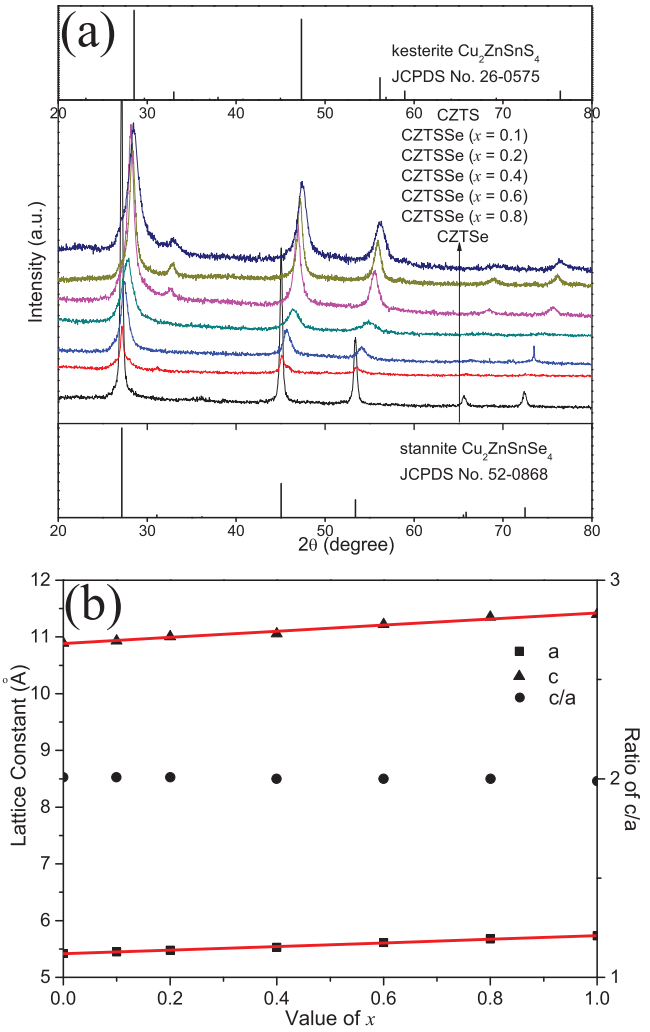

Figure 1 | (a) XRD diffraction peaks, and (b) lattice constant of CZTSSe nanocrystals with different contents of Se.

Results

Synthesis and characterizations of compositionally tunable CZTSSe nanocrystals with high phase purity. Powders of as-synthesized nanocrystals were submitted to X-ray diffraction (XRD) characterization for phase identification. Figure 1a shows XRD patterns of the as-synthesized CZTSSe nanocrystals. Increasing the content of Se from 0% to 100%, the phase of CZTSSe nanocrystals changes smoothly from kesterite CZTS to stannite CZTSe, revealed from the gradual downward shift of the diffraction peaks to lower angles. The shift of the diffraction peaks is because of the enlarged interplanar spacings after incorporating bigger Se atoms. The lattice constant (a and c) increases linearly with the content of Se (x value) as shown in Fig. 1b. No additional peaks from secondary phases could be observed. To further confirm the phase purity of CZTSSe nanocrystals, Raman characterization of CZTSSe nanocrystals were conducted. Raman peaks of CZTSSe nanocrystals are compared in Fig. 2. All peaks of CZTS nanocrystals could be assigned to vibration modes of kesterite CZTS[1,27], with the major one (A_1 mode) centered at 333 cm^{-1}. Peaks from Cu_xS, ZnS, SnS_2 and ternary Cu–Sn–S compounds could not be detected[27], indicating the phase purity of the as-synthesized CZTS nanocrystals. Phase-pured CZTSe nanocrystals have the major A_1 mode centered at 192 cm^{-1} with an additional CZTSe peak centered at 238 cm^{-1}. Increasing the content of Se from 0% to 100%, Raman peak positions move to lower wave numbers and the peaks from CZTS disappear while those from CZTSe dominate. The A_1 peak frequency ratio of CZTS to CZTSe equals approximately to the ratio of the square root of the atomic masses of Se to S, as reported previously[1]. Most importantly, no impurity phases could be identified in the Raman spectra of CZTSSe nanocrystals in their complete composition range.

In order to ascertain the valence states of composing elements and the final composition, the as-synthesized CZTSSe nanocrystals were examined by X-ray photoelectron spectroscopy (XPS). XPS spectra of CZTSSe nanocrystals are shown in Fig. 3 and Fig. S1 and S2. Valence state of Cu and Sn could be determined as Cu^+ and Sn^{4+}, respectively, according to their peak splitting values[28]. The 2p peak of S lying in the range of 160–164 eV suggests its sulfide states[28]. Zn and Se are found to be in their Zn^{2+} and Se^{2-} state[29]. Finally, the surface composition of CZTS nanocrystals could be determined as $Cu_{2.19}Zn_{1.06}SnS_{4.06}$ (Fig. S1). The surface composition of CZTSSe

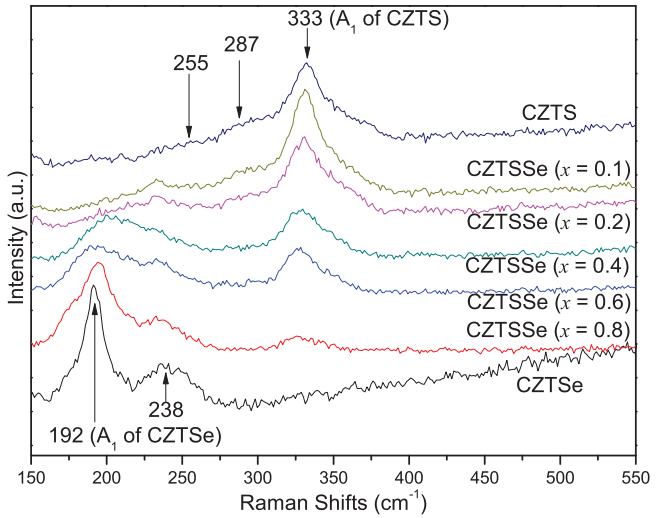

Figure 2 | **Raman peaks of CZTSSe nanocrystals with different contents of Se.**

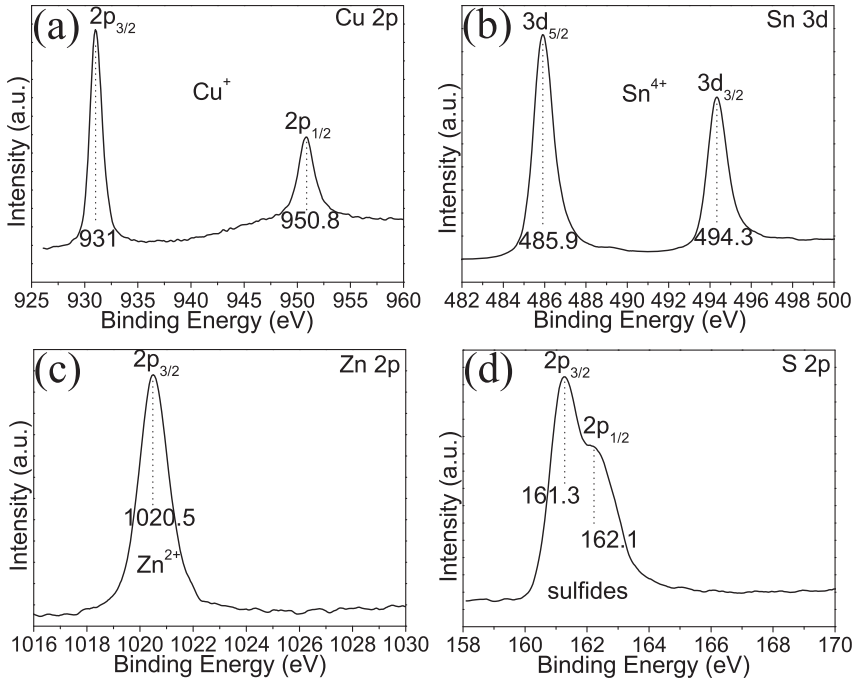

Figure 3 | High-resolution XPS analysis of CZTS nanocrystals.

nanocrystals with a nominal Se content of 20% could be determined as $Cu_{2.14}Zn_{0.96}SnS_{3.2}Se_{0.72}$ (Fig. S2).

Because of the limited penetration depth, XPS could only give surface information of samples. Alternatively, synchrotron-based X-ray absorption has been used to investigate the phase purity and internal structure of the as-synthesized CZTSSe nanocrystals, because of its high penetration depth and extreme sensitivity to local structure. Figure 4a and 4b exhibit the X-ray near-edge structure (XANES) at Cu and Zn *K*-edges for CZTSSe nanocrystals with Cu_2S and ZnS as the reference. All the curves of the as-synthesized samples are vividly different from that of Cu_2S and ZnS, excluding the existence of these two phases. To clarify the cause of differences between CZTSSe samples, we carried out XANES simulations taking into account of two structure models for Cu and Zn *K*-edge. The calculated XANES spectra by using the *Feff8.4 code*[30] are also shown in Fig. 4a and 4b. The main features of Cu and Zn *K*-edge XANES spectra of CZTSSe ($x = 0.1$) and CZTSSe ($x = 0.8$) were well reproduced by corresponding models, indicating that the origin of different curve shapes is structural change, instead of secondary phases. In other words, all Se atoms replace S atoms in the parent lattice, and CZTSSe samples change from kesterite to stannite structure with increasing the content of Se. Figure 4c and 4d display the radial distribution functions of Cu and Zn *K*-edge extended X-ray absorption fine structure for CZTSSe with different Se contents. It is clearly shown that the CZTSSe lattice is expanded with the increase of the content of Se, agreeing well with Fig. 1b.

To reveal their morphology, CZTSSe nanocrystals were characterized by transmission electron microscopy (TEM) (Fig. 5). CZTSSe nanocrystals are highly crystallized and could be dispersed in hexane. Interplanar spacings from high-resolution TEM (HRTEM) and TEM electron diffraction patterns were in accordance with those obtained by XRD. Analysis by energy dispersive spectrometer (EDS) confirmed the existence of Cu, Zn, Sn, S, Se and their stoichiometry was close to that ascertained by XPS (Fig. S3). To test compositional uniformity among nanocrystals, we synthesized CZTSe crystals with large size and performed EDS mapping on them as shown in Fig. S4. Distributions of each element corresponded well with crystal morphology, which manifested the compositional uniformity.

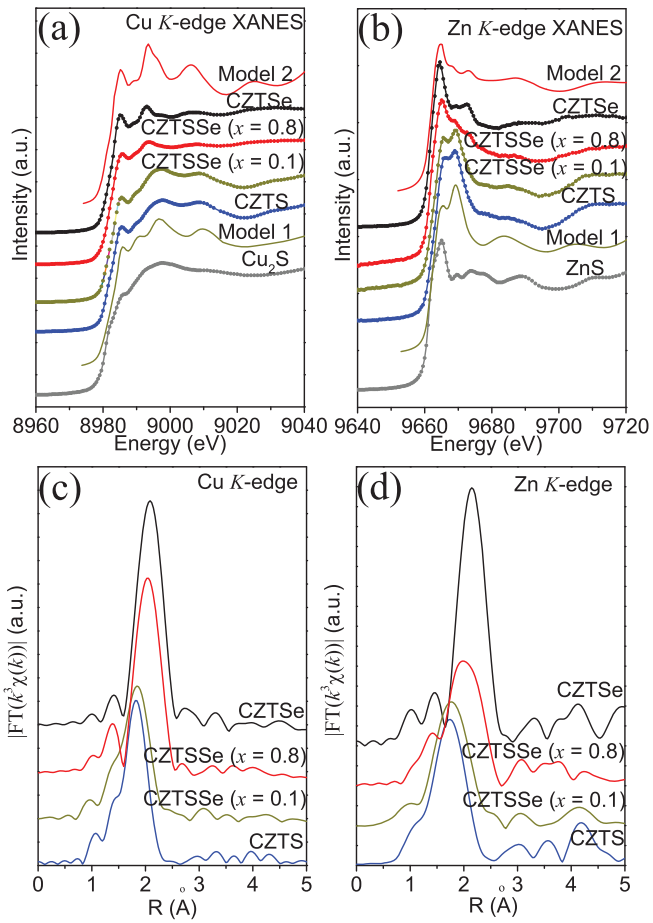

Figure 4 | X-ray absorption spectra of CZTSSe nanocrystals.

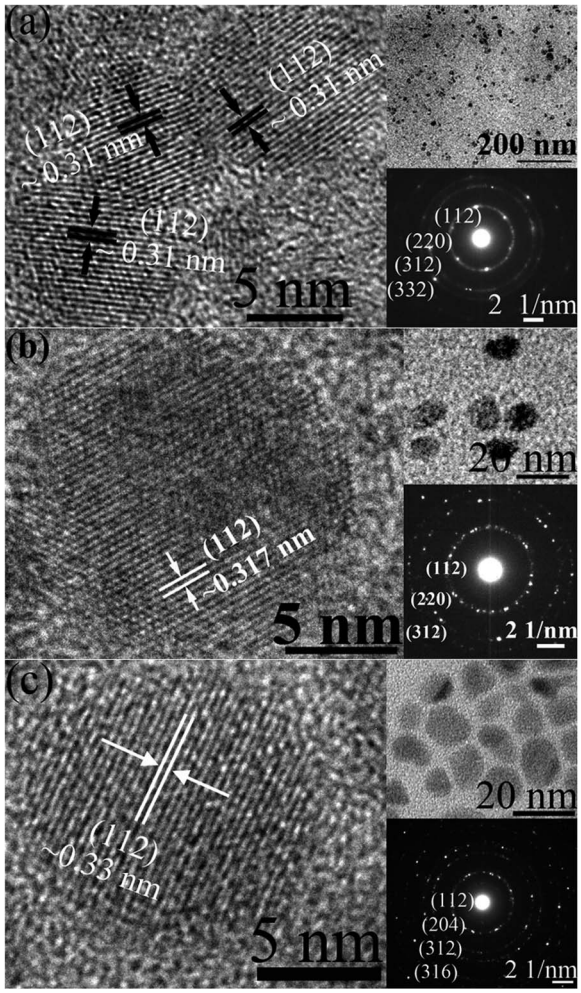

Figure 5 | TEM characterizations of CZTSSe nanocrystals. (a) CZTS, (b) CZTSSe ($x = 0.2$), (c) CZTSe.

Composition-related energy band of CZTSSe nanocrystals. Bandgap of CZTSSe nanocrystals were determined to be direct from Tauc equation fitting of experimental absorbance and values were obtained (Fig. 6 and Fig. S5). As a consequence of the compositional tunability, bandgap of CZTSSe nanocrystals could be manipulated from 1.5 eV to 1.12 eV. The variation of the bandgap with the content of Se (x value) could be modeled by Végard's law, described by the equation of $E_g(x) = (1 - x)E_g(\text{CZTS}) + xE_g(\text{CZTSe}) - bx(1 - x)$, where the bowing constant, b, describing the extent of nonlinearity, gave the value of ~0.06 eV (Fig. 6b). This value is similar to the values of CZTSSe (0.07 eV) and $CuIn(S_{1-x}Se_x)_2$ (0.04 eV) from theoretical results[31,32]. We noticed that the bandgap of CZTSe was suggested to be around 1.0 eV by theoretical calculations[31] and intensive experimental work[33], instead of being close to 1.5 eV as suggested in the early literature. The small deviation of the bandgap values in the present work might be due to the uncertainty in fitting the absorbance curves using Tauc equation. With the bandgap of CZTSSe nanocrystals changing from 1.5 eV to 1.12 eV, conduction band minimum determined from cyclic voltammetry scan (Fig. 6 and Fig. S6) is lowed from −3.9 eV (relative to vacuum energy) to −4.61 eV by increasing the Se/S ratio. Valence band maximum is settled between −5.4 eV and −5.73 eV. The cyclic voltammetry results are in accordance with those of ultraviolet photoelectron spectroscopy (UPS) as shown in Fig. S7.

Discussion

As a multicomponent compound, CZTSSe are usually accompanied with impurities of ternary and binary chalcogenides whose crystal structures and lattice constants are close to each other. Accurate control of the incorporating amount of Se atoms into kesterite structure of CZTS is a challenge due to the difference between anion atoms and accompanied cation disorders usually observed in stannite CZTSe. It poses dramatic difficulty in phase control and phase identification. In the present work, the lattice constant increasing linearly with the incorporation of Se and the constant c/a ratio manifest the successful synthesis of phase pure CZTSSe nanocrystals in their complete composition range without severe distortion of the tetragonal structure (Fig. 1). Considering the adjacency of XRD diffraction peaks between CZTSSe phase and impurity phases like ZnS(Se) and ternary Cu–Sn–S(Se), Raman analysis is commonly applied to further test the phase purity of CZTSSe. The absence of peaks from vibration modes of these impurity phases and gradually changing of Raman spectrum from CZTS to CZTSe is another piece of evidence for the phase purity of CZTSSe nanocrystals. XPS is surface sensitive and helps us to identify surface composition segregation through values of valence state and stoichiometry of each element. No variable valence states are observed and the compositions of as-synthesized CZTSSe nanocrystals are nearly stoichiometric. It excludes the existence of surface segregated phases like Cu_xS, which usually appears by high temperature synthetic method. In contrast to XPS, technique of synchrotron-based X-ray absorption could give internal structure information and ascertain the phase purity of samples due to its high penetration depth and extreme sensitivity to local structure. From experimental and theoretical spectra analysis, no secondary phases whether on the surface or in the internal exist. Structural change from kesterite type of CZTS to stannite type of CZTSe is evidenced and complete composition range of CZTSSe nanocrystals is confirmed once more.

To reveal its role in controlling the phase purity of CZTSSe nanocrystals played by OLA, mixture of different volume ratios of OLA and glycerol were used as solvents. Interestingly, we found that instead of a pure OLA solvent, a volume content of OLA as small as 20–30% was sufficient for the preparation of phase pure CZTSSe nanocrystals. For preparation of CZTS nanocrystals, decreasing the volume content below 10%, cubic Cu_2SnS_3 dominated the product (Fig. S9). When glycerol was used as the sole solvent, Cu_2SnS_3 and other impurity phases were obtained (Fig. S9b). The Raman spectrum of Cu_2SnS_3 synthesized by 10% volume content of OLA was given for comparison (Fig. S9d). It is clearly different from that of CZTS as shown in Fig. 2. For successful synthesis of multicomponent nanocrystals, high reaction temperature, sufficient contact among each element precursor and effective capping of products to inhibit rapid growth are necessary. Glycerol, a low-cost and common organic solvent with boiling point as high as 290°C, could provide high reaction temperature and reducing atmosphere protecting products from oxidation, which has been demonstrated for the synthesis of noble metal or chalcogenide nanocrystals[34,35]. The binding ability of OH groups also helps to complex with metal elements and to cap products[36]. As a result, the key to phase control of CZTSSe is to choose appropriate amount of complexing agent (OLA, for example) guaranteeing sufficient alloying of each precursor. To incorporate bigger Se atoms into CZTS nanocrystals, larger volume content of OLA and/or higher reaction temperature was needed. As is well known, the S precursor and the Se precursor in colloidal synthesis usually show different reactivity[22], so larger amount of complexing agent is needed to form Se precursor which could help to balance the reactivity between these two precursors. Take CZTSe as an example, at least 30% volume content of OLA was required for guaranteeing the phase purity.

Amines with short chain length, are promising candidates as the solvent in synthesizing nanocrystals, because with short chain length molecues, ligand exchange may be not a necessity[26]. We have examined the replacement of OLA with ethylenediamine. We could still obtain phase pure CZTS nanocrystals, although the homogeneity of

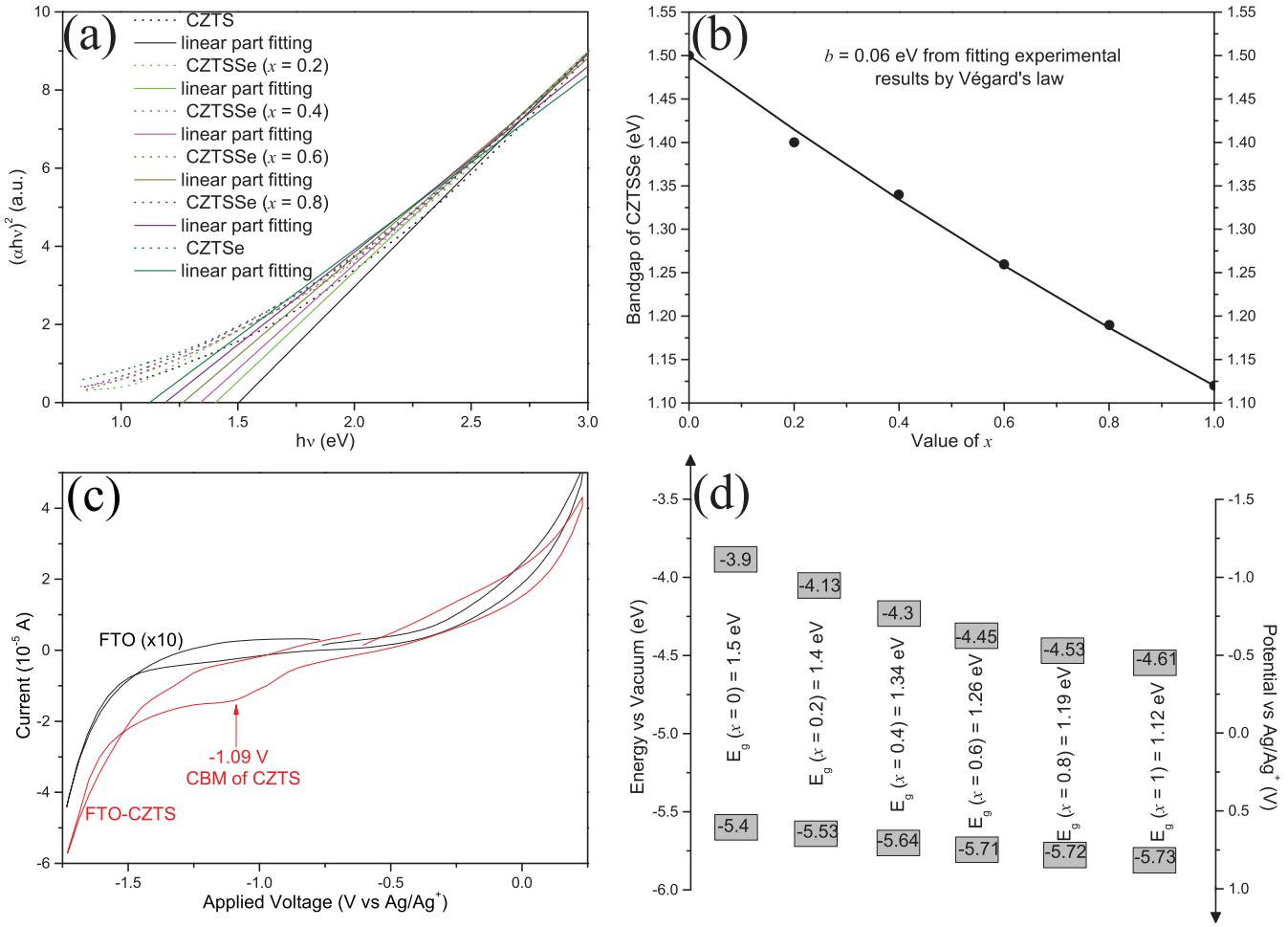

Figure 6 | Energy bands of CZTSSe nanocrystals. (a) Experimental bandgap determined from fitting normalized absorbance of CZTSSe nanocrystals according to Tauc equation, (b) dependence of experimental bandgap on CZTSSe composition and its theoretical fitting by Végard's law, (c) cyclic voltammetry scan of CZTS nanocrystal film, (d) scheme of energy levels of CZTSSe nanocrystals deduced from their respective cyclic voltammetry scan and optical bandgap test.

shape and size of the as-synthesized nanocrystals is not as good as when OLA was used (Fig. S10–S12). However, it is possible to add other short-chain molecules to adjust the morphology and size of the nanocrystals, which entails further work.

From the above analysis, we can conclude that phase pure CZTSSe nanocrystals in their complete composition range have been synthesized. Consequently, bandgap of as-synthesized CZTSSe nanocrystals changes linearly with the composition, giving a small Végard's

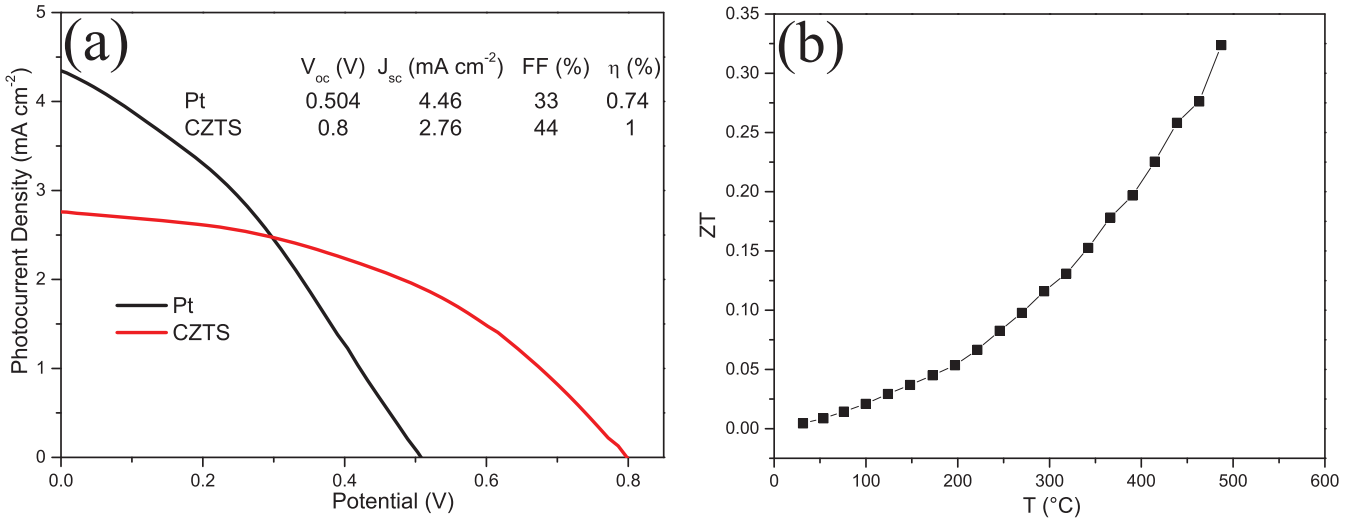

Figure 7 | Application tests of untreated CZTSSe nanocrystals. (a) Electrocatalytic test of CZTS nanocrystals in a traditional CdS-sensitized TiO_2 solid-liquid junction solar cell with Pt sheet as reference, (b) thermoelectric test of CZTSe nanocrystals.

bowing parameter of ~0.06 eV, which is close to zero. The nearly linear decrease of the bandgap with the content of Se agrees well with that predicted by Wei and coworkers[31], which is another piece of evidence for the composition tunability and the phase controllability of CZTSSe nanocrystals in this work. Most important of all, graded energy levels of conduction and valence bands of CZTSSe nanocrystals are verified from chemical cyclic voltammetry method which is in accordance with results of physical UPS method. Band alignment among CZTSSe nanocrystals will help to facilitate charge separation and transport when constructing rainbow solar cells for further increase the efficiency of state of the art CZTSSe solar cells.

CZTSSe nanocrystals synthesized by the solution route developed in this work are not heavily coated with long-chain OLA and sufficiently washed, so carrier transport among these nanocrystals without additional ligand exchange or heating would not be a problem. Acturally as device fabrication is considered, solution methods are better than high-temperature, vacuum-based processing on cost reduction and feasible phase control[37,38]. This is projected by forming CZTSSe films simply from low temperature spinning or sparying. The CZTS nanocrystals were used as electrocatalysts in a traditional CdS-sensitized TiO_2 solid-liquid junction solar cell using polysulfide redox couple. Figure 7a presents the comparing results with CZTS film as counter electrode improving the cell efficiency. Open-circuit voltage was increased from 0.5 V in Pt catalyzed solar cell to 0.8 V in CZTS catalyzed one, which could be ascribed to suppressing the overpotential for charge transfer on the surface of CZTS. To further explore their excellent electronic performance, thermoelectric test was done on CZTSSe nanocrystals. CZTSe nanocrystals were hot-pressed into a tablet which was cut into two parts for individual electric and thermal tests. ZT value of about 0.35 at 500°C could be obtained (Fig. 7b). Recently, Yu group have synthesized non-stoichiometric CZTSe nanocrystals in 10 g scale using OLA and obtained respectable ZT value[10]. In our first example for the thermoelectric properties, we have already shown that the device performance was comparable to that of PbSe:Na synthesized by high temperature sintering[20]. Further work on optimizing the thermoelectric performance is underway. The green, economic and scalable route developed here makes it possible to make use of waste heat by these nontoxic and earth-abundant CZTSSe materials.

In conclusion, CZTSSe nanocrystals have been synthesized by an economic route. The composition of CZTSSe nanocrystals could be tuned from pure CZTS to pure CZTSe with a good reproducibility. As a consequence of the composition tunability, the optical bandgap of the nanocrystals could also be tuned in a large range. Meanwhile, conduction band edges were shifted apparently and valence band edges almost unchanged. The feasible energy band manipulation in this work is critically important to couple the materials to the solar spectrum by constructing rainbow solar cells and also useful for efficient electrocatalysis. Electrocatalytic activity towards polysulfide redox couple by CZTS nanocrystals outperformed that of expensive Pt. Thermoelectric test of CZTSe nanocrystals gave a relative high ZT value of ~0.35 at 500°C. Therfore, CZTSSe nanocrystals synthesized in this work will find a wide range of applications, including thermoelectrics and photovoltaics.

Methods

Material synthesis. Gram-scale $Cu_2ZnSn(S_{1-x}Se_x)_4$ nanocrystals were synthesized by the colloid chemical method employing mixed solvents of glycerol and OLA (For details see Supplementary Methods online). Briefly, stoichiometric amount of CuCl, $ZnCl_2$, $SnCl_4$, elemental S and Se were loaded into a 250-mL three-neck flask with certain volume of glycerol and OLA. The flask was heated under stirring in an Ar atmosphere firstly to a temperature for precursor complexing and then to the final temperature for reaction. After reaction, products were separated by centrifugation by adding ethanol and washed with dichloromethane. Colloid of nanocrystals in hexane was prepared for electron-microscopy characterization and powder was vacuum dried for further characterizations. As a supplemental experiment, OLA in the above synthetic procedure was replaced by the same amount of ethylenediamine, where other conditions were kept unchanged. The purifying procedure was similar but only ethanol was used.

Material characterizations. CZTSSe nanocrystals were submitted to in-depth combined optical and structural characterizations including TEM, EDS, XRD, Raman, XPS, UPS, XANES, Absorption and CV. For application tests, electrocatalytic activity of CZTS film was compared with Pt sheet and thermoelectric performance of CZTSe tablet was evaluated (For details see Supplementary Methods online).

Structure related XANES simulation. We carried out XANES simulations taking into account of two structure models for Cu and Zn *K*-edge. The structure of Model 1 is Se atom substituting for S atom partially in the first shell with the kesterite structure. The structure of Model 2 is substitutional S at part of Se site near absorption atoms in the stannite structure. The XANES spectra were calculated by using the *Feff8.4 code*[30].

1. Mitzi, D. B., Gunawan, O., Todorov, T. K., Wang, K. & Guha, S. The path towards a high-performance solution-processed kesterite solar cell. *Sol. Energy Mater. Sol. Cells* **95**, 1421–1436 (2011).
2. Todorov, T. K. *et al.* Beyond 11% Efficiency: Characteristics of State-of-the-Art $Cu_2ZnSn(S,Se)_4$ Solar Cells. *Adv. Energy Mater.* **3**, 34–38 (2013).
3. Fan, F. *et al.* Linearly arranged polytypic CZTSSe nanocrystals. *Sci. Rep.* **2**, 952 (2012).
4. Ji, S. & Ye, C. Cu_2ZnSnS_4 as a New Solar Cell Material: The History and the Future. *Rev. Adv. Sci. Eng.* **1**, 42–58 (2012).
5. Xin, X., He, M., Han, W., Jung, J. & Lin, Z. Low-Cost Copper Zinc Tin Sulfide Counter Electrodes for High-Efficiency Dye-Sensitized Solar Cells. *Angew. Chem. Int. Ed.* **50**, 11739–11742 (2011).
6. Xu, J., Yang, X., Yang, Q., Wong, T. & Lee, C. Cu_2ZnSnS_4 Hierarchical Microspheres as an Effective Counter Electrode Material for Quantum Dot Sensitized Solar Cells. *J. Phys. Chem. C* **116**, 19718–19723 (2012).
7. Cao, Y. *et al.* Highly Electrocatalytic $Cu_2ZnSn(S_{1-x}Se_x)_4$ Counter Electrodes for Quantum-Dot-Sensitized Solar Cells. *ACS Appl. Mater. Interfaces* **5**, 479–484 (2013).
8. Yang, H., Jauregui, L. A., Zhang, G., Chen, Y. P. & Wu, Y. Nontoxic and Abundant Copper Zinc Tin Sulfide Nanocrystals for Potential High-Temperature Thermoelectric Energy Harvesting. *Nano Lett.* **12**, 540–545 (2012).
9. Liu, M., Huang, F., Chen, L. & Chen, I. A wide-band-gap *p*-type thermoelectric material based on quaternary chalcogenides of Cu_2ZnSnQ_4 (Q = S, Se). *Appl. Phys. Lett.* **94**, 202103 (2009).
10. Fan, F., Wang, Y., Liu, X., Wu, L. & Yu, S. Large-Scale Colloidal Synthesis of Non-Stoichiometric $Cu_2ZnSnSe_4$ Nanocrystals for Thermoelectric Applications. *Adv. Mater.* **24**, 6158–6163 (2012).
11. Haight, R. *et al.* Band alignment at the $Cu_2ZnSn(S_xSe_{1-x})_4$/CdS interface. *Appl. Phys. Lett.* **98**, 253502 (3 pages) (2011).
12. MacDonald, B. I. *et al.* Layer-by-Layer Assembly of Sintered $CdSe_xTe_{1-x}$ Nanocrystal Solar Cells. *ACS Nano* **6**, 5995–6004 (2012).
13. Ruland, A., Schulz-Drost, C., Sgobba, V. & Guldi, D. M. Enhancing Photocurrent Efficiencies by Resonance Energy Transfer in CdTe Quantum Dot Multilayers: Towards Rainbow Solar Cells. *Adv. Mater.* **23**, 4573–4577 (2011).
14. Kaczmarek, M. & Bredol, M. Electrocatalytic activity of undoped and Mn-doped Zn(S, Se)-carbon nanocomposites. *J. Mater. Sci.* **46**, 5400–5405 (2011).
15. Lee, H. J. *et al.* Regenerative PbS and CdS Quantum Dot Sensitized Solar Cells with a Cobalt Complex as Hole Mediator. *Langmuir* **25**, 7602–7608 (2009).
16. Zeier, W. G. *et al.* Phonon Scattering through a Local Anisotropic Structural Disorder in the Thermoelectric Solid Solution $Cu_2Zn_{1-x}Fe_xGeSe_4$. *J. Am. Chem. Soc.* **135**, 726–732 (2013).
17. Xiao, C. *et al.* High Thermoelectric and Reversible *p-n-p* Conduction Type Switching Integrated in Dimetal Chalcogenide. *J. Am. Chem. Soc.* **134**, 18460–18466 (2012).
18. Chen, S., Gong, X. G., Walsh, A. & Wei, S. Electronic structure and stability of quaternary chalcogenide semiconductors derived from cation cross-substitution of II-VI and I-III-VI_2 compounds. *Phys. Rev. B* **79**, 165211 (2009).
19. Pei, Y., Wang, H. & Snyder, G. J. Band Engineering of Thermoelectric Materials. *Adv. Mater.* **24**, 6125–6135 (2012).
20. Zhao, L. *et al.* High Thermoelectric Performance via Hierarchical Compositionally Alloyed Nanostructures. *J. Am. Chem. Soc.* **135**, 7364–7370 (2013).
21. Pei, Y. *et al.* Convergence of electronic bands for high performance bulk thermoelectrics. *Nature* **473**, 66–69 (2011).
22. Riha, S. C., Parkinson, B. A. & Prieto, A. L. Compositionally Tunable $Cu_2ZnSn(S_{1-x}Se_x)_4$ Nanocrystals: Probing the Effect of Se-Inclusion in Mixed Chalcogenide Thin Films. *J. Am. Chem. Soc.* **133**, 15272–15275 (2011).
23. Ou, K. *et al.* Hot-injection synthesis of monodispersed $Cu_2ZnSn(S_xSe_{1-x})_4$ nanocrystals: tunable composition and optical properties. *J. Mater. Chem.* **22**, 14667–14673 (2012).
24. Nag, A. *et al.* Metal-free Inorganic Ligands for Colloidal Nanocrystals: S^{2-}, HS^-, Se^{2-}, HSe^-, Te^{2-}, HTe^-, TeS_3^{2-}, OH^-, and NH_2^- as Surface Ligands. *J. Am. Chem. Soc.* **133**, 10612–10620 (2011).
25. Jiang, C., Lee, J. & Talapin, D. V. Soluble Precursors for $CuInSe_2$, $CuIn_{1-x}Ga_xSe_2$, and $Cu_2ZnSn(S,Se)_4$ Based on Colloidal Nanocrystals and Molecular Metal Chalcogenide Surface Ligands. *J. Am. Chem. Soc.* **134**, 5010–5013 (2012).
26. Fischer, A. *et al.* Directly Deposited Quantum Dot Solids Using a Colloidally Stable Nanoparticle Ink. *Adv. Mater.* http://dx.doi.org/10.1002/adma.201302147.

27. Fernandes, P. A., Salomé, P. M. P. & Cunha, A. F. Study of polycrystalline Cu_2ZnSnS_4 films by Raman scattering. *J. Alloy. Compd.* **509**, 7600–7606 (2011).
28. Pawar, B. S. *et al.* Effect of complexing agent on the properties of electrochemically deposited Cu_2ZnSnS_4 (CZTS) thin films. *Appl. Surf. Sci.* **257**, 1786–1791 (2010).
29. Danilson, M. *et al.* XPS study of CZTSSe monograin powders. *Thin Solid Films* **519**, 7407–7411 (2011).
30. Stern, E. A., Newville, M., Ravel, B., Yacoby, Y. & Haskel, D. The UWXAFS analysis package: philosophy and details. *Physica B* **208 & 209**, 117–120 (1995).
31. Chen, S. *et al.* Compositional dependence of structural and electronic properties of $Cu_2ZnSn(S,Se)_4$ alloys for thin film solar cells. *Phys. Rev. B* **83**, 125201 (2011).
32. Wei, S. & Zunger, A. Band offsets and optical bowings of chalcopyrites and Zn-based II-VI alloys. *J. Appl. Phys.* **78**, 3846–3856 (1995).
33. Ahn, S. *et al.* Determination of band gap energy (E_g) of $Cu_2ZnSnSe_4$ thin films: On the discrepancies of reported band gap values. *Appl. Phys. Lett.* **97**, 021905 (2010).
34. Yu, Q., Liu, C., Zhang, Z. & Liu, Y. Facile Synthesis of Semiconductor and Noble Metal Nanocrystals in High-Boiling Two-Phase Liquid/Liquid Systems. *J. Phys. Chem. C* **112**, 2266–2270 (2008).
35. Tüysüz, H., Liu, Y., Weidenthaler, C. & Schüth, F. Pseudomorphic Transformation of Highly Ordered Mesoporous Co_3O_4 to CoO via Reduction with Glycerol. *J. Am. Chem. Soc.* **130**, 14108–14110 (2008).
36. Dong, W., Yen, S., Paik, J. & Sakamoto, J. The Role of Acetic Acid and Glycerol in the Synthesis of Amorphous MgO Aerogels. *J. Am. Ceram. Soc.* **92**, 1011–1016 (2009).
37. Scragg, J. J., Ericson, T., Kubart, T., Edoff, M. & Platzer-Björkman, C. Chemical Insights into the Instability of Cu_2ZnSnS_4 Films during Annealing. *Chem. Mater.* **23**, 4625–4633 (2011).
38. Repins, I. *et al.* Co-evaporated $Cu_2ZnSnSe_4$ films and devices. *Sol. Energy Mater. Sol. Cells* **101**, 154–159 (2012).

Acknowledgments

This work was supported by National Basic Research Program of China (973 Program, Grant No. 2011CB302103), National Natural Science Foundation of China (Grant Nos. 11074255 and 11274308), and the Hundred Talents Program of the Chinese Academy of Sciences. We thank beamline BL14W1 (Shanghai Synchrotron Radiation Facility) for providing the beam time.

Author contributions

S.J. and C.Y. contributed to the conception and design of the experiment, analysis of the data and writing the manuscript. X.Q. and C.C. assisted S.J. by carrying out synthesis of materials, optical and structural characterizations of the synthesized products. J.Z. performed the experiment of thermoelectricity conversion and G.X. carried out electrocatalytic test. T.S. and S.J. did synchrotron-based X-ray absorption tests and analyzed the results with assistance of Z.J.

Additional information

Supplementary information accompanies this paper at http://www.nature.com/scientificreports

Competing financial interests: The authors declare no competing financial interests.

How to cite this article: Ji, S. *et al.* A Route to Phase Controllable $Cu_2ZnSn(S_{1-x}Se_x)_4$ Nanocrystals with Tunable Energy Bands. *Sci. Rep.* **3**, 2733; DOI:10.1038/srep02733 (2013).